MIT Libraries | DSpace@MIT

MIT Open Access Articles

Impact of sour gas composition on ignition delay and burning velocity in air and oxy-fuel combustion

The MIT Faculty has made this article openly available. ***Please share*** how this access benefits you. Your story matters.

Citation: Bongartz, Dominik and Ghoniem, Ahmed F. "Impact of Sour Gas Composition on Ignition Delay and Burning Velocity in Air and Oxy-Fuel Combustion." Combustion and Flame 162, no. 7 (July 2015): 2749–2757 © 2015 The Combustion Institute

As Published: http://dx.doi.org/10.1016/j.combustflame.2015.04.014

Publisher: Elsevier

Persistent URL: http://hdl.handle.net/1721.1/109914

Version: Author's final manuscript: final author's manuscript post peer review, without publisher's formatting or copy editing

Terms of use: Creative Commons Attribution

Massachusetts Institute of Technology

© 2015. This manuscript version is made available under the CC-BY-NC-ND 4.0 license.
Accepted for Publication in Combustion and Flame, April 2015
Published article: http://dx.doi.org/10.1016/j.combustflame.2015.04.014

Impact of sour gas composition on ignition delay and burning velocity in air and oxy-fuel combustion

Dominik Bongartz[1], Ahmed F. Ghoniem*

Department of Mechanical Engineering, Massachusetts Institute of Technology, 77 Massachusetts Avenue, Cambridge, MA 02139, USA

Abstract

Sour gas is an unconventional fuel consisting mainly of methane (CH_4), carbon dioxide (CO_2), and hydrogen sulfide (H_2S) that constitutes a considerable, currently untapped energy source. However, little is known about its combustion characteristics. In this work, we used our recently assembled and validated detailed chemical reaction mechanism to examine some of the combustion properties of sour gas with different compositions in both conventional air combustion and oxy-fuel combustion, the latter being motivated by application in carbon capture and storage. The calculations suggest that raising the H_2S content in the fuel leads to relatively small changes in the flame temperature and laminar burning velocity, but a considerable reduction in the ignition delay time. At elevated pressures, H_2O diluted oxy-fuel combustion leads to higher burning velocities than CO_2 diluted oxy-fuel combustion or air combustion. Mixed CH_4/H_2S flames exhibit a two-zone structure in which H_2S is oxidized completely to sulfur dioxide (SO_2) while CH_4 is converted to carbon monoxide (CO). Formation of corrosive sulfur trioxide (SO_3) mainly occurs during CO burnout.

Keywords: sour gas, hydrogen sulfide, sulfur oxidation, oxy-fuel combustion, kinetic mechanisms, premixed flames

1. Introduction

Sour gas is a special type of natural gas that is currently not being used as a fuel because it contains significant fractions (up to 30% by volume [1]) of hydrogen sulfide (H_2S) and carbon dioxide (CO_2) and so far requires energy-intensive and expensive gas clean-up. Since sour gas resources are significant [2] and there is increasing interest in natural gas as a cleaner alternative to coal for power generation, it is becoming increasingly attractive to develop technologies to overcome this difficulty. One strategy is to use sour gas directly in a gas turbine process employing an oxy-fuel combustion (or oxy-combustion) strategy, possibly combined with enhanced oil recovery. This could help address issues associated with the formation of highly corrosive sulfur trioxide (SO_3) and the low heating value caused by the high CO_2 contents in the fuel [3–5].

However, very little is known about the characteristics of sour gas as a fuel. In particular, it is not known how different compositions of sour gas affect flame stabilization characteristics or flame structure. There has also been a dearth of experimental information on H_2S oxidation, by itself or as part of a mixture with methane (CH_4). This is the case for conventional air combustion, but certainly even more so for oxy-combustion with its unusual combustion environment consisting of pure oxygen (O_2) and either CO_2 or water (H_2O) as diluents. As a starting point to address this need, we recently assembled and validated a chemical kinetics mechanism for the combustion of H_2S and mixtures of CH_4 of H_2S [3].

*Corresponding author. 77 Massachusetts Avenue, Room 3-344, Cambridge MA 02139, USA. Fax: +1-617-253-5981. Phone: +1-617-253-2295.

Email addresses: dominikbongartz@alum.mit.edu (Dominik Bongartz), ghoniem@mit.edu (Ahmed F. Ghoniem)

[1]Present address: AVT Process Systems Engineering, RWTH Aachen University, Turmstrasse 46, 52064 Aachen, Germany.

The purpose of this paper is therefore to predict some fundamental properties of sour gas combustion under different conditions by means of detailed chemical kinetics calculations, coupled with the corresponding transport properties in the case of premixed flames. The goal is to characterize the influence of varying the fuel composition and to identify possible differences between the different combustion modes (i.e. air combustion vs. CO_2 or H_2O diluted oxy-combustion) based on the observed chemical pathways. We first briefly describe the models used and the parameter ranges considered in the study. Next, we summarize our predictions for the adiabatic flame temperature, ignition delay time, laminar burning velocity, and premixed flame structure of sour gas in air and oxy-fuel combustion using CO_2 or H_2O dilution. Finally, we draw some conclusions for the design of gas turbine combustors burning sour gas.

2. Modeling

The chemical reaction mechanism for sour gas combustion employed in this study is presented in detail in reference [3]. It is a combination of the AramcoMech 1.3 mechanism for the combustion of small hydrocarbons by Metcalfe et al. [6] with an optimized version of the recent mechanism for H_2S oxidation developed by Zhou et al. [7]. The overall mechanism consists of 157 species and 1011 reactions. It has been validated for oxy-fuel combustion of CH_4, air combustion of H_2S, and important interactions between carbon and sulfur species. The scope of the validation was determined by the availability of experimental data [3].

All calculations were conducted in CHEMKIN-PRO [8], using the equilibrium model for the adiabatic flame temperature, the homogeneous reactor model with constant pressure for the ignition delay time, and the flame speed analyzer for the laminar burning velocity and the flame structure calculations. For flame calculations, thermal diffusion of species (the Soret effect) had to be considered.

For the present analysis, sour gas was assumed to be a mixture of CH_4 and H_2S only. The H_2S mole fraction in the fuel was varied between 0% and 30% to account for the range of common sour gas compositions [1]. Carbon dioxide in the fuel was not considered for simplicity, since its influence can be inferred from the calculations for oxy-fuel combustion using CO_2 dilution.

In air combustion, the equivalence ratio Φ was considered as a variable (design) parameter. For oxy-fuel combustion, the equivalence ratio was fixed at $\Phi = 1$, since oxy-fuel systems are likely to operate neither fuel-lean nor fuel-rich to avoid wasting energy for O_2 production or fuel, respectively [9, 10]. In this case, the diluent mole fraction can be adjusted instead, since unlike in air combustion the oxidizer and diluent contents are independent.

3. Adiabatic Flame Temperature

In air combustion, the adiabatic flame temperature can be varied by changing the equivalence ratio. In oxy-combustion, it is controlled by the diluent mole fraction since the equivalence ratio is fixed at $\Phi \approx 1$ (cf. Section 2). For simplicity, we only considered atmospheric pressure without preheating ($p = 1$ atm, $T_{\mathrm{in}} = 300$ K). The same qualitative trends also apply at elevated pressure and temperature.

Regardless of the combustion mode, the flame temperature decreases by about 30-50 K when raising the H_2S content in the fuel from 0% to 30% (see Fig. 1). This is caused by the smaller lower heating value (LHV) of H_2S, which according to calculations using the same thermochemical data is only 65% of the heating value of CH_4 ($\mathrm{LHV}_{\mathrm{H_2S}} = 518$ kJ/mol as compared to $\mathrm{LHV}_{\mathrm{CH_4}} = 803$ kJ/mol).

In the case of oxy-fuel combustion, the adiabatic flame temperature is higher when using H_2O as a diluent as compared to CO_2. This difference can be explained with the higher isobaric heat capacity (c_{p}) of CO_2 (e.g. $c_{p,\mathrm{CO_2}} = 58.4$ J/molK at $T = 1500$ K as compared to $c_{p,\mathrm{H_2O}} = 47.1$ J/molK).

4. Ignition Delay Time

The ignition delay time is a common metric for describing the oxidation characteristics of a fuel and can give some indications of flame stabilization behavior. If the fuel is to be used in a gas turbine employing premixed combustion, the ignition delay time is important in determining the possibility of autoignition that can damage the equipment [11].

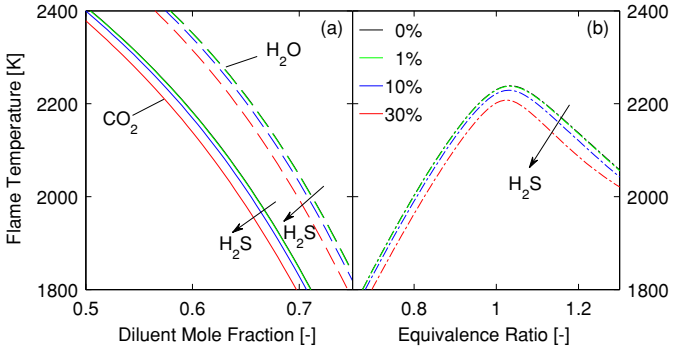

Figure 1: The adiabatic flame temperature of sour gas decreases with increasing H_2S content in the fuel: (a) Oxy-fuel combustion with CO_2 dilution (solid lines) and H_2O dilution (dashed lines), (b) Air combustion.

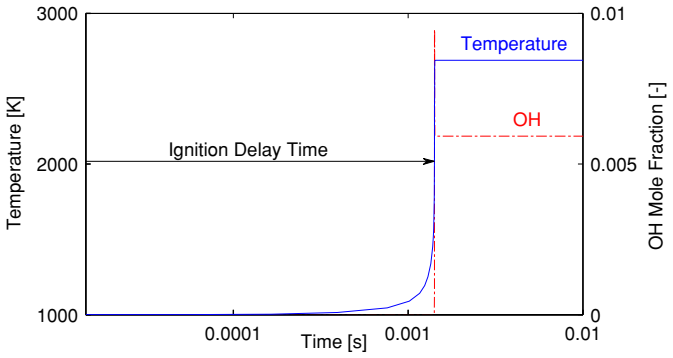

Figure 2: Definition of the ignition delay time by the temperature inflection point. The OH mole fraction is shown for comparison. Sour gas (30% H_2S, 70% CH_4) in air at $\Phi = 1$, $p = 40$ atm, $T_0 = 1000$ K.

For the present analysis, we defined the ignition delay time using the temperature inflection point (see Fig. 2). However, the results presented here are not sensitive to the exact definition of the ignition delay time. For all cases, we considered a constant pressure of $p = 40$ atm and an initial temperature of $T_0 = 800$-1200 K. We decided to use constant pressure rather than constant volume simulations in order to account for the fact that in gas turbine combustors, pressure typically stays constant within a few percent [11]. The values of pressure and temperature are chosen to be representative of the inlet conditions of gas turbine combustors, but also close enough to the conditions for which the H_2S kinetics are validated [3]. However, preliminary calculations at different pressures between $p = 1$ atm and $p = 80$ atm revealed the same qualitative trends.

4.1. Impact of Fuel Composition

The ignition delay time of sour gas in air decreases with increasing H_2S content in the fuel, indicating that the low and intermediate temperature kinetics of the mixture get faster (see Fig. 3). At low temperature ($T_0 \approx 800$ K), addition of only 1% H_2S already lead to a substantial decrease (-65%) in the ignition delay time as compared to pure CH_4. Higher concentrations of H_2S further decrease the ignition delay time only slightly (up to -83% for pure H_2S as compared to pure CH_4). At higher temperature ($T_0 \approx 1200$ K), however, the promoting effect of small concentrations of H_2S is less pronounced while higher concentrations have a stronger promoting effect than at lower temperature. The same qualitative behavior was also observed for oxy-fuel combustion using CO_2 or H_2O dilution (not shown here).

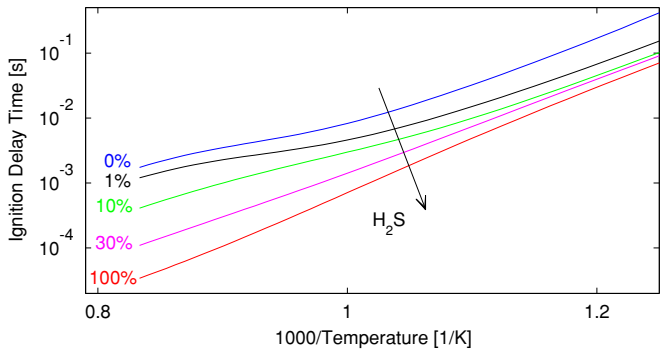

Figure 3: The ignition delay time of sour gas decreases with increasing H_2S mole fraction in the fuel (air combustion at $\Phi = 1$ and $p = 40$ atm).

Addition of H_2S has a significant impact on the radical pool. Compared to pure CH_4, small amounts of H_2S lead to a much faster buildup of H, OH, HO_2, and in particular O (see Fig. 4, note the different timescales in the two subfigures). It also enhances the conversion of HO_2 to H_2O_2, especially in the early stages. The relative importance of these changes in enhancing ignition depends on the temperature and the H_2S content of the fuel.

The increased size of the radical pool can be explained by the high reactivity of intermediate sulfur species. In the early stages, H_2S is mostly consumed by the reaction

$$H_2S + HO_2 \leftrightarrow SH + H_2O_2, \tag{R1}$$

which especially at low temperature is significantly faster (e.g. almost 1,300 times faster at $T = 800$ K) than the corresponding carbon reaction

$$CH_4 + HO_2 \leftrightarrow CH_3 + H_2O_2. \tag{R2}$$

As the OH concentration rises, the reaction

$$H_2S + OH \leftrightarrow SH + H_2O \tag{R3}$$

gets increasingly important too (see Fig. 5). The mercapto radicals (SH) formed through reactions R1 and R3 quickly react in the chain propagating reactions

$$SH + HO_2 \leftrightarrow HSO + OH \tag{R4}$$

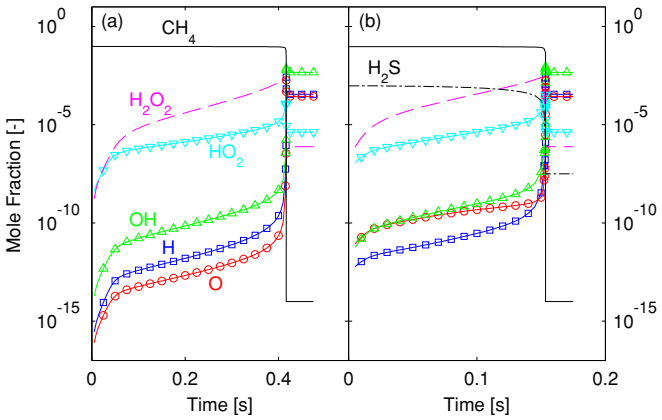

Figure 4: The ignition delay of pure CH_4 in air at $T_0 = 800$ K (a). Addition of 1% H_2S to the fuel (b) results in faster formation of radicals (in particular O atoms) as well as H_2O_2. Note the different time scales. $\Phi = 1$ and $p = 40$ atm.

$$SH + O_2 \leftrightarrow SO_2 + H, \tag{R5}$$

which compete with the chain terminating reaction

$$SH + HO_2 \leftrightarrow H_2S + O_2. \tag{R6}$$

Reactions R4 and R5 lead to a rise in the concentrations of OH and H, respectively. The HSO formed in reaction R4 further reacts in the branching sequence (cf. Fig. 5)

$$HSO + O_2 \leftrightarrow SO + HO_2 \tag{R7}$$

$$HSO + HO_2 \leftrightarrow SO + H_2O_2 \tag{R8}$$

$$SO + O_2 \leftrightarrow SO_2 + O. \tag{R9}$$

Even for addition of only 1% H_2S, reaction R9 becomes the dominant formation reaction for O atoms in the early stages (e.g. for the conditions of Fig. 4b, it is responsible for more than 90% of the O atom formation at any given time throughout 95% of the ignition delay). The rise in the conversion of HO_2 to H_2O_2 in the presence of H_2S is mostly due to reaction R1 and (to a lesser extent) reaction R8.

It is well known [12–16] that the ignition of hydrocarbons at high pressure and intermediate temperature is controlled by the formation of OH radicals via the chain branching reaction

$$H_2O_2(+M) \leftrightarrow OH + OH(+M). \tag{R10}$$

In the context of the present study, the enhanced formation of OH radicals through reaction R4 and the faster buildup of H_2O_2 is thus expected to be particularly important for small H_2S mole fractions (mostly hydrocarbon ignition) and low temperature ($T \leq 1000$ K [12]), which is confirmed by sensitivity analyses (see Fig. 6 and also the sensitivity analysis for ignition of pure H_2S in [3]). In particular, the importance of the competition between reactions R4 and R6 and the is evident at low temperature ($T_0 \approx 800$ K). At higher temperature ($T_0 \approx 1200$ K), the importance of reaction R10 is reduced, and ignition is now mainly controlled by the competition of the chain terminating reaction

$$CH_3 + CH_3(+M) \leftrightarrow C_2H_6(+M) \tag{R11}$$

with reactions leading to CH_3O or CH_2O (see Fig. 6).

The higher O atom concentration caused by the branching sequence R7-R9 (which is also initiated by reaction R4) promotes ignition by providing branching H abstraction reactions for stable species like CH_4, CH_2O, and (at higher

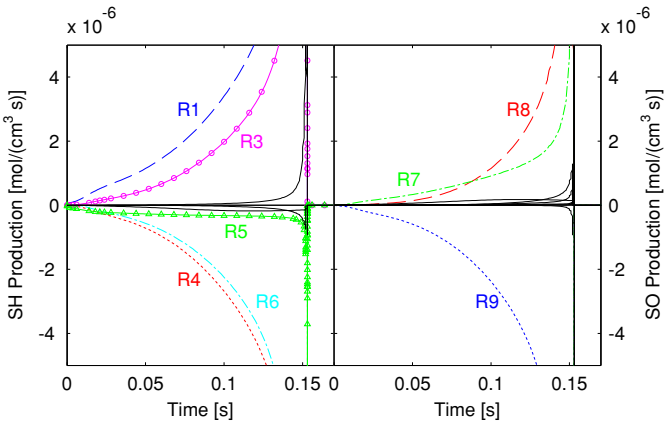

Figure 5: In low temperature ignition, SH is mostly formed via $H_2S+HO_2=SH+H_2O_2$ (R1) and $H_2S+OH=SH+H_2O$ (R3) and quickly reacts via $SH+O_2=SO_2+H$ (R5), $SH+HO_2=HSO+OH$ (R4), or $SH+HO_2=H_2S+O_2$ (R6). The HSO produced in R4 is converted to SO via $HSO+O_2=SO+HO_2$ (R7) and $HSO+HO_2=SO+H_2O_2$ (R8). The oxidation of SO via $SO+O_2=SO_2+O$ (R9) is a major source of O atoms. Same conditions as Fig. 4b, vertical axis was cropped for better readability.

temperature) C_2H_6. This effect gets stronger as the H_2S mole fraction is increased further and the branching sequence based on the self reaction of SH becomes more important:

$$SH + SH \leftrightarrow H_2S + S \tag{R12}$$

$$S + O_2 \leftrightarrow SO + O \tag{R13}$$

$$SO + O_2 \leftrightarrow SO_2 + O \tag{R9}$$

This sequence was first described by Zhou et al. [7] and can also be seen in the sensitivity analyses in our previous work [3].

Note that a promoting effect of H_2S in high pressure, intermediate temperature ignition was also observed in a numerical study of syngas combustion by Mathieu et al. [17] using a similar mechanism [18]. They stated that H_2S only enhances ignition at conditions where HO_2 is the dominant radical species, which however is clearly the case in the present study (see Fig. 6) and thus is not a contradiction.

4.2. Impact of the Combustion Mode

When comparing the different combustion modes (i.e. air combustion vs. CO_2 or H_2O diluted oxy-combustion), a distinction has to be made as to whether we simply replace nitrogen (N_2) in air with CO_2 or H_2O (i.e. we have a fixed diluent mole fraction in the oxidizer $X_{dil,ox} = 0.79$), which leads to different flame temperatures for a given initial temperature and fuel composition, or we always adjust the CO_2 or H_2O mole fraction in order to match the flame temperature of the air combustion case.

In either case, we observe that the influence of the combustion mode is much less significant than that of the fuel composition. If the comparison is made at the same diluent mole fraction, oxy-fuel combustion with CO_2 dilution leads to the longest ignition delay time for both CH_4 and H_2S (see Fig. 7a), as well as any mixture between the two (not shown). At high temperature, air combustion leads to the lowest ignition delay, while at lower temperature (T_0 = 800 K) H_2O provides the fastest ignition. If, on the other hand, the comparison is made at equal flame temperature, air combustion leads to an ignition delay that is about a factor of 1.5 longer than the two oxy-combustion modes (see Fig. 7b). Again, H_2O gives the shortest ignition delay at low temperatures while at higher temperature CO_2 leads to the shortest ignition delay.

This behavior can be explained by the different thermodynamic and chemical kinetic properties of the different diluents. To demonstrate these effects, we conducted calculations similar to those shown in Fig. 7a, but with fictitious, inert versions of the diluents denoted vN_2, vCO_2, and vH_2O. These species have the same thermodynamic (and

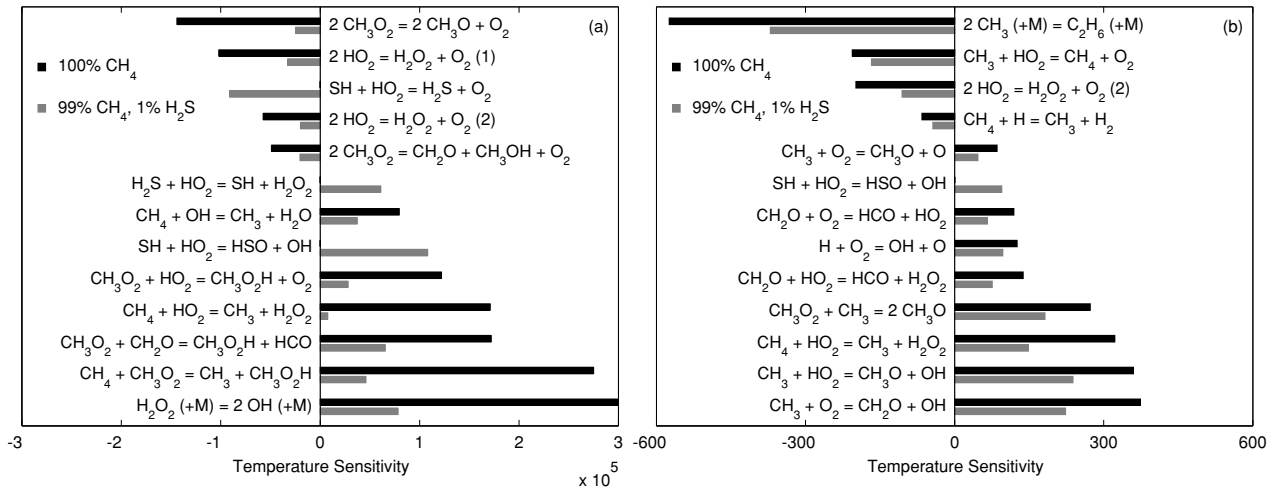

Figure 6: Sensitivity of temperature to the pre-exponential factors of important reaction rates during the ignition of pure CH_4 and sour gas with 1% H_2S in the fuel. Air combustion at $\Phi = 1$ and $p = 40$ atm. (a) $T_0 = 800$ K, (b) $T_0 = 1200$ K.

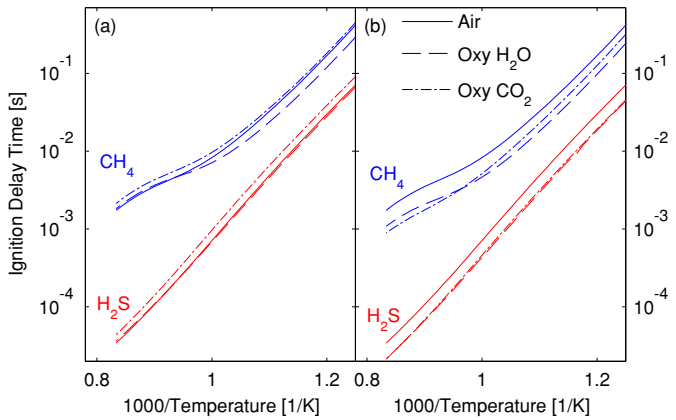

Figure 7: The change in the ignition delay time of sour gas (for any composition, bracketed by CH_4 and H_2S) when changing the combustion mode depends on how the comparison is made: (a) Constant diluent mole fraction ($X_{dil} = 0.79$ in the oxidizer). (b) Constant flame temperature (X_{dil} is adjusted to match the temperature of the air case).

transport) properties as the original species, but do not participate as reactants in any chemical reactions and are assigned a third body efficiency of one (analogous to, e.g., Liu et al. [19]).

When comparing at the same diluent mole fraction, the different heat capacities of the diluents lead to different flame temperatures (cf. Section 3). Hence, the thermodynamic properties of the diluent have a tendency to increase the ignition delay time in the order of their (molar) isobaric heat capacities, i.e. $vCO_2 > vH_2O > vN_2$ (see Fig. 8a).

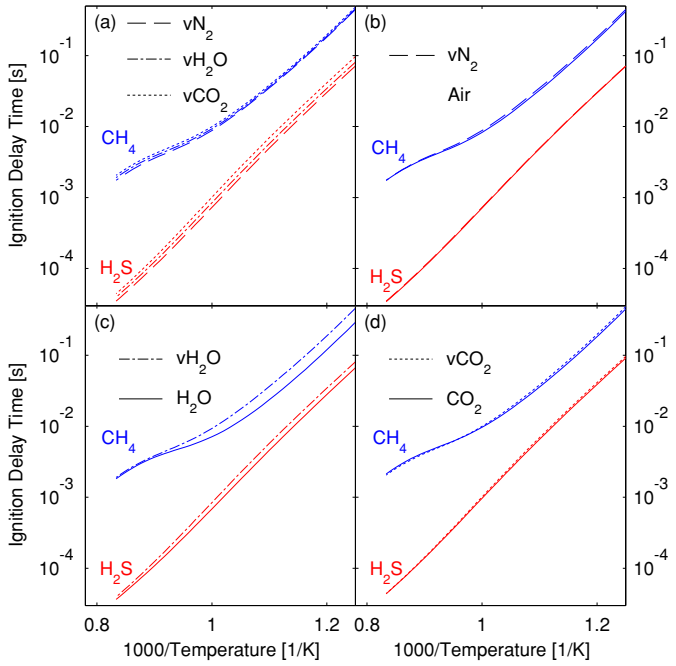

Figure 8: The ignition delay time of sour gas (bracketed by CH_4 and H_2S) at $p = 40$ atm at $\Phi = 1$ is influenced by chemical and dilution effects when exchanging the diluent. (a) When chemical effects are removed, the ignition delay time is determined by different heat capacities. (b) N_2 has almost no chemical effect. (c) The chemistry of H_2O decreases the ignition delay. (d) CO_2 has almost no chemical effect.

For all three diluents, there is an ignition-enhancing chemical effect through the participation of the (reactive) diluents as a third body in the chain branching reaction R10. This effect is stronger for CH_4 than for H_2S and it is particularly pronounced below $T_0 \approx 1000$ K, which are the conditions under which reaction R10 controls ignition (cf. Section 4.1). For N_2 and CO_2, this effect is relatively weak (see Fig. 8b and 8d) since their third body efficiencies for this reaction are only 1.5 and 1.6, respectively. In the case of CO_2, it is even partially offset by the ability of CO_2 to dissociate and thus decrease the flame temperature. Water, on the other hand, has a much higher third body efficiency of about seven for reaction R10 so that the decrease in the ignition delay time is much stronger (see Fig. 8c). This explains why the curve of the ignition delay time in the presence of H_2O in Fig. 7a is essentially shifted down relative to the other two, especially at lower temperature.

For interpreting the behavior at equal flame temperature (Fig. 7b), we note that in this case the influence of the thermodynamics are opposite to the previous case: since CO_2 has the highest heat capacity, less of it has to be added to achieve a given flame temperature than when using H_2O or N_2 as a diluent. Therefore, the concentrations of fuel and oxidizer are higher (although the equivalence ratio always remains fixed at $\Phi = 1$), which tends to decrease the ignition delay time.

5. Laminar Burning Velocity

The laminar burning velocity gives valuable insight into flame stabilization characteristics. As in Section 3, the degrees of freedom are the H_2S mole fraction in the fuel and the equivalence ratio for air combustion or the diluent mole fraction for oxy-fuel combustion. Unless otherwise stated we only considered atmospheric pressure

without preheating, since the high-temperature H_2S kinetics are not validated at elevated pressure because of a lack of experimental data.

5.1. Impact of Fuel Composition

For air combustion and CO_2 diluted oxy-fuel combustion, the burning velocity decreases slightly for small H_2S mole fraction and increases over the initial value for larger H_2S mole fractions (see Fig. 9a). For H_2O diluted oxy-combustion, there is a continuing decrease in the burning velocity up to pure H_2S.

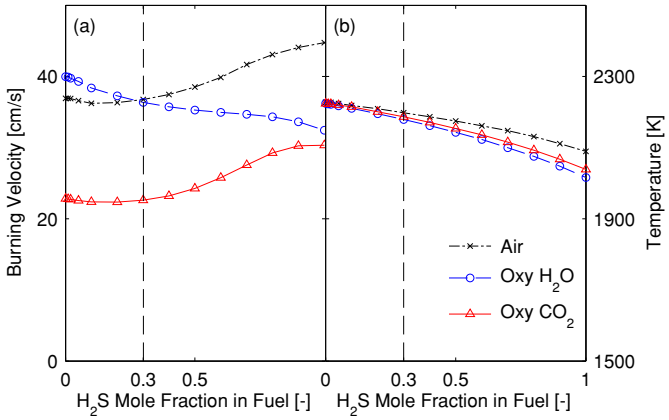

Figure 9: For a fixed equivalence ratio of $\Phi = 1$ and diluent mole fraction ($X_{CO_2} = 0.578$ for CO_2 dilution and $X_{H_2O} = 0.646$ for H_2O dilution), the burning velocity (a) and flame temperature (b) show a different behavior with changing H_2S content for the different combustion modes. Typical sour gas compositions are to the left of the dashed line.

The inhibiting effect at low H_2S mole fractions with an increase of the burning velocity at higher mole fractions for air combustion has been observed experimentally by Kurz [20] for propane-H_2S-air flames. This is caused by two separate chemical effects.

The slight decrease in the burning velocity when adding small amounts of H_2S is due to the fact that the sulfur dioxide (SO_2) formed catalyzes H and OH radical removal through the reactions

$$H + SO_2(+M) \leftrightarrow HOSO(+M) \quad \text{(R14)}$$

$$HOSO + H \leftrightarrow SO^* + H_2O, \quad \text{(R15)}$$

where SO^* denotes the singlet state of SO, which quickly reacts further via

$$SO^* + M \leftrightarrow SO + M \quad \text{(R16)}$$

$$SO + OH \leftrightarrow SO_2 + H \quad \text{(R17)}$$

$$SO + O_2 \leftrightarrow SO_2 + O \quad \text{(R9)}$$

$$SO^* + O_2 \leftrightarrow SO_2 + O. \quad \text{(R18)}$$

Reaction R14 is the only sulfur reaction with a significant sensitivity for the laminar burning velocity at low H_2S contents, and if it is removed from the mechanism, the inhibiting effect does indeed disappear. This sequence corresponds to a net removal of H and OH radicals through the mechanism described by Rasmussen et al. [21], although the chain terminating effect is weaker if reactions R9 or R18 are involved. Sequences similar to R14-R18 are well known to inhibit the oxidation of CO in the presence of SO_2 [22–25]. Zachariah and Smith [26] also concluded from their experimental and numerical results that SO_2 reduces the flame speed of H_2 flames through a similar mechanism. Although in the present case we add H_2S and not SO_2 to the flame, this mechanism is still important since the oxidation of H_2S to SO_2 occurs early on in the flame (see Section 6.1).

When the H_2S mole fraction is increased further, the kinetics of H_2S oxidation itself become more important and the burning velocity increases for air combustion and CO_2 diluted oxy-fuel combustion as it approaches that of pure H_2S (e.g. for air combustion at $\Phi = 1$ we have $s_{L,CH_4} = 37$ cm/s and $s_{L,H_2S} = 45$ cm/s). For H_2O dilution, the burning velocity of pure H_2S at these conditions is smaller than the one of CH_4 so that the decrease in the burning velocity continues. The chemical effects that are responsible for this behavior are discussed in Section 5.2.

It should be noted that within the range of H_2S mole fractions that are common for sour gas (0 to 30%), the variation in the laminar burning velocity is relatively small (cf. Fig. 9a). If the concomitant decrease in the flame temperature is compensated by adjusting the equivalence ratio (for air combustion) or the diluent mole fraction (for oxy-combustion), the inhibiting effect around 0 to 10% H_2S gets even smaller, and addition of 30% H_2S leads to an increase in the burning velocity under most conditions.

5.2. Impact of the Combustion Mode

In order to make a fair comparison between the different combustion modes (air vs. oxy-combustion with CO_2 or H_2O dilution), we investigated the burning velocity as a function of the adiabatic flame temperature. For brevity, we mainly discuss pure CH_4, but the same effects are observed for H_2S or mixtures between the two fuels as well.

For a given flame temperature, air combustion gives the highest burning velocity except around $T_{\text{flame}} = 2200$-2250 K, followed by oxy-fuel combustion with H_2O dilution, while CO_2 dilution gives the lowest values (see Fig. 10d). To highlight what causes this behavior, we conducted several additional calculations.

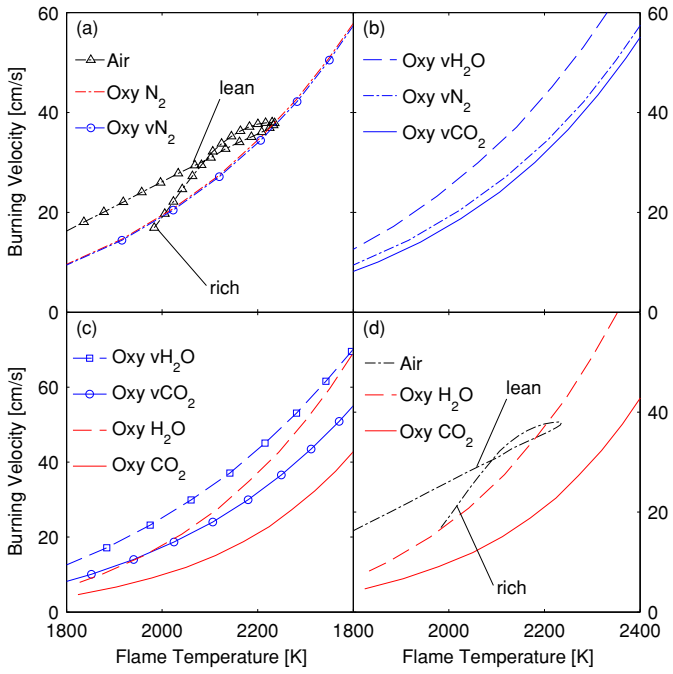

Figure 10: The influence of different effects on the laminar burning velocity of CH_4 at $p = 1$ atm. (a) Air combustion compared to combustion in O_2 and N_2 or O_2 and vN_2 (=inert N_2) with fixed $\Phi = 1$ and varying diluent concentration. (b) Oxy-fuel combustion using inert versions of N_2, CO_2, and H_2O as diluents, showing the influence of the transport properties. (c) Comparison of combustion using the inert and real diluents, showing the chemical effect of the diluents. (d) Comparison of the three relevant combustion modes.

First, we compared the burning velocity of CH_4/air flames at different equivalence ratios to that of $CH_4/O_2/N_2$ flames at $\Phi = 1$ while varying the N_2 mole fraction in the latter (labeled 'Oxy N_2'), as well as flames with the virtual molecule 'vN_2' (cf. Section 4.2) that has the same properties as N_2 but does not participate in any reactions (see Fig. 10a). The air flames are faster than the Oxy N_2 flames because in cases where $\Phi \neq 1$ the 'diluent' consists not only of virtually inert N_2, but also either excess O_2 or fuel. It can be seen that the chemistry of N_2 has virtually no influence on the laminar burning velocity.

A comparison of the burning velocity of oxy-fuel flames with inert N_2 to similar flames using inert CO_2 ('vCO_2') and H_2O ('vH_2O') highlights the influence of the diluents' transport properties, since the diluents do not participate in any reactions (and hence do not influence the radical pool) and comparison is made at the same flame temperature (see Fig. 10b). The transport properties of H_2O lead to an increase in the burning velocity relative to N_2 whereas the properties of CO_2 lead to a slight decrease. The relative change in the burning velocity corresponds roughly to the square root of the change in the diffusion coefficient for H radicals in the respective diluent, which is consistent with the scaling commonly derived from simplified analyses with single step kinetics (see, e.g., Turns [27]). As an example, at $T = 2000$ K this diffusion coefficient is increased by 27% in H_2O as compared to N_2 but decreased by 11% in CO_2.

Both CO_2 and H_2O have chemical effects that slow down the kinetics, with CO_2 leading to the stronger inhibition (see Fig. 10c). This is in agreement with the results in the literature [19, 28–31]. For CO_2, the inhibition is mainly caused by the reaction

$$H + CO_2 \leftrightarrow OH + CO, \tag{R19}$$

which competes with the main chain branching reaction

$$H + O_2 \leftrightarrow OH + O, \tag{R20}$$

as was first observed by Liu et al. [19]. For H_2O, as was observed in [30–32], there is an inhibition due to the high third body efficiency of H_2O in the reaction

$$H + O_2(+M) \leftrightarrow HO_2(+M), \tag{R21}$$

which also competes with the main chain branching reaction R20. To a lesser extent, this is also true for CO_2, which in the present mechanism is assigned a third body efficiency of 3.8 for reaction R21 as compared to 10 for H_2O and 1 for N_2. The inhibiting chemical effect of H_2O is partially counteracted by the enhancement of the branching reaction

$$HCO + M \leftrightarrow H + CO + M, \tag{R22}$$

for which the third body efficiency of H_2O is set to 12 (as compared to 2 for CO_2 and 1 for N_2) [33].

The same qualitative observations regarding the different thermal, transport, and chemical effects were also made for pure H_2S (not shown here), the only exception being a much stronger inhibiting chemical effect of H_2O (cf. also Section 5.1). This stronger inhibition is partly due to the fact that H_2O is a very efficient third body in reaction R14 that is responsible for the SO_2 catalyzed radical removal described in Section 5.1. Addition of H_2O also impacts the radical pool via

$$H_2O + O \leftrightarrow OH + OH, \tag{R23}$$

leading to lower O and higher OH concentrations [33–35]. The former inhibits the reaction

$$S_2 + O \leftrightarrow SO + S \tag{R24}$$

that can initiate the branching reactions R13 and R9, while the latter enhances the chain propagating reaction R17 that competes for SO with the branching R9. Furthermore, H_2O also acts as an efficient third body in the chain terminating reaction

$$SO + O(+M) \leftrightarrow SO_2(+M). \tag{R25}$$

Finally, the branching reaction R22 that is enhanced by the addition H_2O does not occur in the absence of hydrocarbons. As a consequence of these effects, the burning velocity of H_2S at a given flame temperature is almost equal for CO_2 and H_2O diluted oxy-fuel combustion (cf. also Fig. 9).

5.3. Influence of Pressure

For all fuel compositions and combustion modes, the burning velocity decreases significantly when raising the pressure from 1 atm to 20 atm and changes only relatively little with further increases in pressure (see Fig. 11), corresponding to the expected power law $s_L \propto p^{(n-2)/2}$ (see, e.g., Turns [27]), where s_L is the laminar burning velocity and n is the overall reaction order.

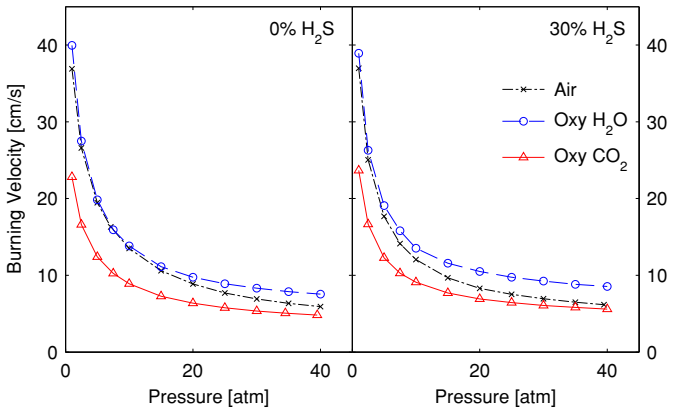

Figure 11: The burning velocity of CH_4 decreases faster with pressure for air combustion at $\Phi = 1$ than for oxy-combustion at $\Phi = 1$ with CO_2 dilution ($X_{CO_2} = 0.578$) or H_2O dilution ($X_{H_2O} = 0.646$).

The pressure dependence is stronger for air combustion ($n \approx 0.95$) than for oxy-combustion ($n \approx 1.10$ for H_2O and $n \approx 1.17$ for CO_2 dilution) and gets only slightly stronger (n is about 3% lower) for the case with 30% H_2S as compared to pure CH_4. As a consequence, at elevated pressures H_2O diluted oxy-combustion leads to the highest burning velocities while air combustion and CO_2 diluted oxy-combustion give similar values that are substantially lower. This is in agreement with the observations of Amato et al. [36], who showed experimentally that CO_2 diluted oxy-fuel CH_4 flames blow off much more easily than air flames at atmospheric pressure, but predicted that their behavior gets more similar at elevated pressures.

However, when interpreting these results we have to keep in mind that there is higher uncertainty in the reaction mechanism at elevated pressure, since for H_2S, data on the burning velocity at increased pressure is lacking altogether and the mechanism was only validated at atmospheric pressure [3]. Thus, the present results should only be seen as qualitative trends.

6. Premixed Flame Structure

To gain further insight into the combustion characteristics, it is useful to investigate not only the burning velocity but also the structure of laminar premixed flames. We only discuss air combustion here, since the only significant effects in oxy-fuel combustion as compared to air combustion that we observed have been reported in the literature before. Namely, these are a rise in CO and a drop in H_2 mole fractions for CO_2 diluted oxy-combustion, and slightly lower CO and higher H_2 for H_2O diluted oxy-combustion [37–40].

6.1. General Structure

To demonstrate the general structure of a sour gas flame (i.e. a flame in which CH_4 and H_2S are oxidized simultaneously), we simulated an air flame with a fuel consisting of 70% CH_4 and 30% H_2S at $\Phi = 0.83$ and atmospheric pressure (see Fig. 12).

The oxidation of the two fuels starts almost simultaneously, but the consumption of H_2S is completed where about 20% of the CH_4 is still present. Similarly, while the first appearance of the final combustion products CO_2 and SO_2 is approximately at the same point, the SO_2 profile is steeper and approaches its final concentration much faster than the CO_2 profile. This is consistent with the observation that the burning velocity of H_2S in air is higher than that of CH_4.

Accordingly, the concentrations of SO as the last intermediate product of H_2S combustion is much lower (even in relation to the initial mole fraction of H_2S) and its peak occurs earlier than for CO, the corresponding carbon species. The peak mole fractions of the only other sulfur compounds occurring in significant amounts, SH and S_2, are another order of magnitude lower and occur slightly before the SO peak, corresponding to their position in the oxidation sequence of H_2S (see, e.g., Zhou et al. [7]). Hydrogen, which appears as an intermediate product of the oxidation of

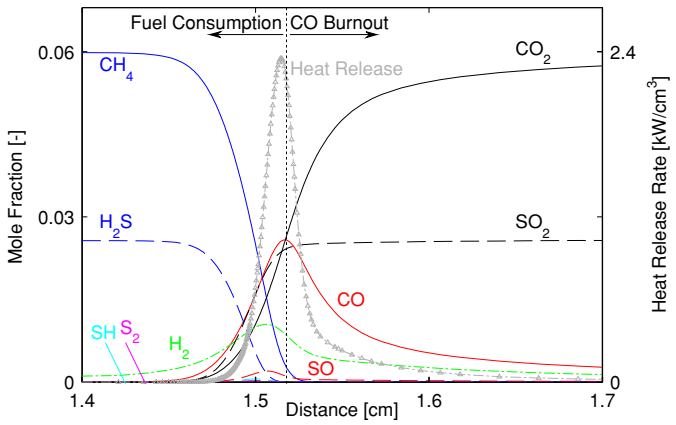

Figure 12: The flame structure of a premixed sour gas-air flame with 30% H_2S in the fuel at $\Phi = 0.83$ and $p = 1$ atm can be divided into two zones (vertical dashed line).

both fuels, has a peak that coincides roughly with the SO peak. The overall heat release rate peaks close to the point where the CH_4 consumption is complete.

Overall, we can identify a two-zone structure similar to the one commonly observed in premixed CH_4-air flames (see, e.g., Turns [27]): In the first zone (labeled 'Fuel Consumption' in Fig. 12), both CH_4 and H_2S are consumed almost entirely. The H_2S is converted virtually completely to SO_2, while the CH_4 forms significant amounts of CO (only about 40% of the carbon are in the form of CO_2 at the end of this zone). While some hydrogen is still present in the form of H_2, the majority (80%) of the H_2O produced in the process is already formed. In the second zone (labeled 'CO Burnout' in Fig. 12), the main reaction occurring is the oxidation of CO to CO_2. Simultaneously, the remaining H_2 is converted to H_2O.

Given the importance of SO_3 because of its role in different corrosion mechanisms, we also investigated the SO_3 profiles, although we expect most of the SO_3 formation in a power plant to occur during the cooling of the flue gas and not in the combustor [41, 42]. Some SO_3 is formed in the flame, corresponding to the equilibrium values at the flame temperature. For all fuel compositions and combustion modes, roughly 0.05% of the total sulfur gets converted to SO_3 (as compared to $O(1\%)$ after cooling in power plants [41]), leading to a maximum concentration of about 30 ppm at the end of the domain for the cases that were considered (occurring for 30% H_2S in the fuel and air combustion).

Virtually all of the SO_3 is formed in the 'CO Burnout' zone (cf. Fig. 12) and the time required to approach the equilibrium concentration is always shorter than the time required for CO oxidation. Only for the highest H_2S content of 30%, the two times are almost equal (see Fig. 13). For modeling purposes, this means that as soon as we assume equilibrium CO at the end of a combustion process, it is a good approximation to also assume equilibrium SO_3. From a practical point of view, it means that CO oxidation and SO_3 will be highly interdependent since they occur on the same time scale, they both depend on the availability of O_2, and they both virtually stop once the temperature drops below $T = 1000$ K [34, 43]. We have confirmed this interdependency in a separate study using a reactor network model of a gas turbine cycle [5].

6.2. Impact of the Fuel Composition

The general flame structure does not change when the H_2S mole fraction in the fuel is varied (see Fig. 14). When the amount of H_2S in the fuel is increased, the concentrations of the sulfur species increases while the concentrations of the carbon species decreases accordingly. The shape of the profiles and the locations of the peaks stay the same except for H_2.

With increasing H_2S content, the H_2 peak gets higher and tends to occur slightly earlier. From the rates of production we can see that the higher H_2 peak is caused by additional H_2 formation mainly through the following reactions:

$$H_2S + H \leftrightarrow SH + H_2 \tag{R26}$$

$$SH + H \leftrightarrow S + H_2 \tag{R27}$$

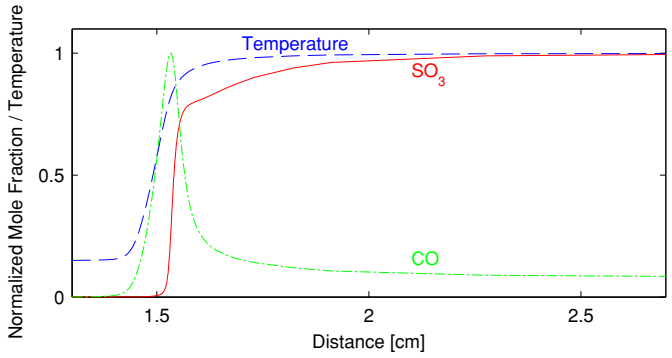

Figure 13: The formation of SO_3 in a H_2O diluted sour gas oxy-fuel flame occurs on the same time scale as the oxidation of CO. The calculations shown are for 30% H_2S in the fuel and combustion at $\Phi = 1$ with $X_{H_2O} = 0.646$, leading to a flame temperature of $T_f = 2000$ K. The mole fractions and the temperature are normalized by their respective maximum value.

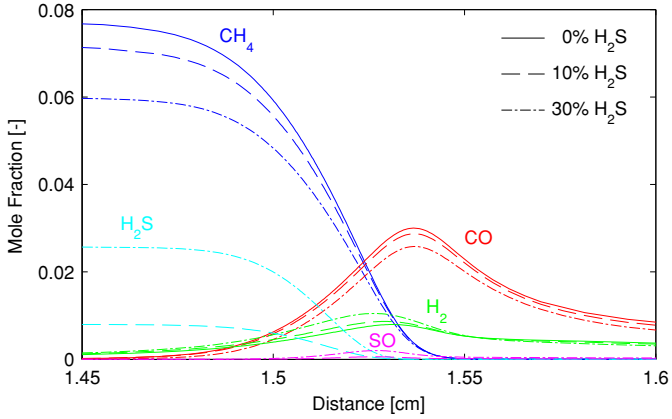

Figure 14: The general flame structure of a premixed sour gas-air flame at $p = 1$ atm does not change with varying H_2S content except for the location of the H_2 peak. The equivalence ratio was adjusted to always give $T_f = 2000$ K.

These occur slightly before the main H_2 formation reactions due to CH_4 oxidation

$$CH_4 + H \leftrightarrow CH_3 + H_2 \tag{R28}$$

$$CH_2O + H \leftrightarrow HCO + H_2, \tag{R29}$$

thus causing the H_2 peak to occur earlier in the flame.

7. Conclusion

A detailed chemical reaction mechanism has been used to predict some fundamental combustion properties of sour gas of varying composition in air and oxy-fuel combustion. We make the following observations about the characteristics of sour gas combustion:

1. Increasing H_2S content in the fuel reduces the adiabatic flame temperature because of the lower heating value of H_2S as compared to CH_4.
2. At the same time, the faster kinetics of H_2S oxidation as compared to CH_4 oxidation lead to a significant drop in the ignition delay time. The ignition delay time changes only slightly between the different combustion modes (air vs. oxy-fuel combustion using CO_2 or H_2O dilution), depending on whether the same diluent mole fraction is used or the same flame temperature.
3. In air combustion and CO_2 diluted oxy-fuel combustion, the laminar burning velocity decreases slightly when adding small amounts ($O(1-10\%)$) of H_2S to CH_4 because the SO_2 formed catalyzes H radical removal. Larger mole fractions of H_2S lead to an increase in the burning velocity. For H_2O diluted oxy-fuel combustion, there is a continuous drop in the burning velocity with increasing H_2S content. For a given flame temperature, the laminar burning velocity at atmospheric conditions is highest for (lean) air combustion and smallest for CO_2 diluted oxy-combustion. At elevated pressures ($\gtrsim$ 10 atm), H_2O diluted oxy-combustion gives the highest burning velocity while air combustion approaches the values for CO_2 dilution.
4. Mixed CH_4 and H_2S flames exhibit a two-zone structure similar to the one found in pure CH_4 flames. The oxidation of H_2S to SO_2 occurs in the same zone as the partial oxidation of CH_4 to CO. In a second zone, CO is converted to CO_2 and simultaneously some SO_2 is further oxidized to SO_3 (on the order of 1–10 ppm), reaching equilibrium on the same time scale.

From these observations, we draw the following conclusions for the design of combustors handling sour gas:

1. Changes in either the flame temperature or the burning velocity due to changing H_2S content in the fuel can be compensated by relatively minor adjustments to the diluent mole fraction (for oxy-combustion) or the equivalence ratio (for air combustion). It thus might be feasible to handle fuels of varying composition in a given combustor, if flashback due to the decreased ignition delay time can be prevented.
2. The oxidation of H_2S can be expected to always go to completion, i.e. no significant amounts of H_2S or intermediate sulfur species are expected in the combustion products. Similar to CO oxidation, formation of corrosive SO_3 will mostly depend on the post-flame conditions.
3. Oxy-fuel combustion with H_2O dilution seems to promise the easiest flame stabilization of the three combustion modes considered here because it leads to the highest burning velocity at relevant pressures.

It should be emphasized, however, that all of these results are modeling predictions, and hence direct experimental validation would be desirable to confirm their validity.

Acknowledgments

The authors gratefully acknowledge the financial support by Siemens Energy, Inc.

References

[1] G. Hammer, T. Lübcke, R. Kettner, M. R. Pillarella, H. Recknagel, A. Commichau, H.-J. Neumann, B. Paczynska-Lahme, in: Ullmann's Encyclopedia of Industrial Chemistry, volume 23, Wiley-VCH, Weinheim, 2012, p. 740.
[2] W. F. J. Burgers, P. S. Northrop, H. S. Kheshgi, J. A. Valencia, Energy Procedia 4 (2011) 2178–2184.
[3] D. Bongartz, A. F. Ghoniem, Combust. Flame 162 (2015) 544–553.
[4] N. W. Chakroun, A. F. Ghoniem, Int. J. Greenh. Gas Control 36 (2015) 1–12.
[5] D. Bongartz, A. F. Ghoniem, Reactor network modeling of sour gas oxy-combustion in gas turbines using detailed kinetics, 2015. Submitted for publication.
[6] W. K. Metcalfe, S. M. Burke, S. S. Ahmed, H. J. Curran, Int. J. Chem. Kinet. 45 (2013) 638–675.
[7] C. Zhou, K. Sendt, B. S. Haynes, Proc. Combust. Inst. 34 (2013) 625–632.
[8] R. J. Kee, F. M. Rupley, J. A. Miller, et al., CHEMKIN-PRO 15112, Reaction Design, San Diego, CA, 2011.
[9] H. M. Kvamsdal, K. Jordal, O. Bolland, Energy 32 (2007) 10–24.
[10] M. B. Toftegaard, J. Brix, P. A. Jensen, P. Glarborg, A. D. Jensen, Prog. Energ. Combust. Sci. 36 (2010) 581–625.
[11] M. Boyce, Gas Turbine Engineering Handbook, Butterworth-Heinemann, Waltham, MA, 4th edition, 2012.
[12] C. K. Westbrook, Proc. Combust. Inst. 28 (2000) 1563 – 1577.
[13] Z. Hong, D. F. Davidson, R. K. Hanson, Combust. Flame 158 (2011) 633 – 644.
[14] D. Healy, D. M. Kalitan, C. J. Aul, E. L. Petersen, G. Bourque, H. J. Curran, Energy Fuels 24 (2010) 1521–1528.
[15] A. Kéromnès, W. K. Metcalfe, K. A. Heufer, N. Donohoe, A. K. Das, C.-J. Sung, J. Herzler, C. Naumann, P. Griebel, O. Mathieu, M. C. Krejci, E. L. Petersen, W. J. Pitz, H. J. Curran, Combust. Flame 160 (2013) 995–1011.
[16] N. Donohoe, A. Heufer, W. K. Metcalfe, H. J. Curran, M. L. Davis, O. Mathieu, D. Plichta, A. Morones, E. L. Petersen, F. Güthe, Combust. Flame 161 (2014) 1432 – 1443.
[17] O. Mathieu, J. Hargis, E. L. Petersen, J. Bugler, H. J. Curran, F. Güthe, in: Proceedings of the ASME Turbo Expo 2014: Turbine Technical Conference and Exposition. June 16-20, 2014, Düsseldorf, Germany, GT2014-25412.
[18] O. Mathieu, F. Deguillaume, E. L. Petersen, Combust. Flame 161 (2014) 23–36.
[19] F. Liu, H. Guo, G. J. Smallwood, Combust. Flame 133 (2003) 495–497.
[20] P. F. Kurz, Ind. Eng. Chem. 45 (1953) 2361–2366.
[21] C. L. Rasmussen, P. Glarborg, P. Marshall, Proc. Combust. Inst. 31 (2007) 339–347.
[22] P. Glarborg, D. Kubel, K. Dam-Johansen, H.-M. Chiang, J. W. Bozzelli, Int. J. Chem. Kinet. 28 (1996) 773–790.
[23] M. U. Alzueta, R. Bilbao, P. Glarborg, Combust. Flame 127 (2001) 2234–2251.
[24] P. Dagaut, F. Lecomte, J. Mieritz, P. Glarborg, Int. J. Chem. Kinet. 35 (2003) 564–575.
[25] J. Giménez-López, M. Martínez, A. Millera, R. Bilbao, M. U. Alzueta, Combust. Flame 158 (2011) 48–56.
[26] M. Zachariah, O. Smith, Combust. Flame 69 (1987) 125–139.
[27] S. R. Turns, An Introduction to Combustion, McGraw-Hill Higher Education, 2000.
[28] V. R. Kishore, N. Duhan, M. R. Ravi, A. Ray, Exp. Therm. Fluid Sci. 33 (2008) 10–16.
[29] F. Halter, F. Foucher, L. Landry, C. Mounaïm-Rousselle, Combust. Sci. Technol. 181 (2009) 813–827.
[30] A. N. Mazas, B. Fiorina, D. A. Lacoste, T. Schuller, Combust. Flame 158 (2011) 2428–2440.
[31] T. Le Cong, P. Dagaut, Energy Fuels 23 (2009) 725–734.
[32] T. Le Cong, P. Dagaut, in: Proceedings of ASME Turbo Expo 2008: Power for Land, Sea and Air. June 9-13, Berlin, Germany, GT2008-50272.
[33] J. Santner, F. Dryer, Y. Ju, Proc. Combust. Inst. 34 (2013) 719–726.
[34] M. Abián, J. Giménez-López, R. Bilbao, M. Alzueta, Proc. Combust. Inst. 33 (2011) 317.
[35] A. Das, K. Kumar, C.-J. Sung, Combust. Flame 158 (2011) 345–353.
[36] A. Amato, B. Hudak, P. D'Carlo, D. Noble, D. Scarborough, J. Seitzman, T. Lieuwen, J. Eng. Gas Turb. Power 133 (2011) 061503.
[37] P. Glarborg, L. L. B. Bentzen, Energy Fuels 22 (2008) 291–296.
[38] H. Watanabe, F. Arai, K. Okazaki, Combust. Flame 160 (2013) 2375–2385.
[39] L. Wang, Z. Liu, S. Chen, C. Zheng, J. Li, Energy Fuels 27 (2013) 7602–7611.
[40] L. Chen, A. F. Ghoniem, Combust. Sci. Technol. 186 (2014) 829–848.
[41] G. Blythe, K. Dombrowski, SO_3 Mitigation Guide Update, Technical Report 1004168, EPRI, Palo Alto, CA, 2004.
[42] D. Fleig, F. Normann, K. Andersson, F. Johnsson, B. Leckner, Energy Procedia 1 (2009) 383–390.
[43] D. Fleig, M. U. Alzueta, F. Normann, M. Abián, K. Andersson, F. Johnsson, Combust. Flame 160 (2013) 1142–1151.